AJR FOCUS ON:

MRI of the Pediatric Knee

Deepa R. Pai[1]
Peter J. Strouse

OBJECTIVE. The purpose of this article is to describe findings on MRI in the evaluation of knee injury in pediatric patients.

CONCLUSION. Injury patterns in the pediatric knee overlap and differ from adults. Differences include open physes, changing mechanics, and differences in ligamentous support. Awareness of normal variants, common incidental findings, and normal evolution of bone marrow aid in the interpretation.

Keywords: child, knee, MRI, pediatrics, trauma

DOI:10.2214/AJR.10.6117

Received November 8, 2010; accepted after revision January 18, 2011.

[1]Both authors: Department of Radiology, Section of Pediatric Radiology, C. S. Mott Children's Hospital, University of Michigan Health System, 1500 E Medical Center Dr, Ann Arbor, MI 48109-0252. Address correspondence to P. J. Strouse (pstrouse@umich.edu).

CME
This article is available for CME credit.
See www.arrs.org for more information.

AJR 2011; 196:1019–1027

0361–803X/11/1965–1019

The knee is the joint most commonly imaged with MRI in the pediatric population. Common indications include assessment of internal derangement, pain, and further investigation of a radiographic abnormality. Although overlap between pediatric and adult pathology exists, particularly in the group of adolescents who have fused growth plates, there are significant differences in the types, prevalence, and underlying mechanism of injuries. The presence of open growth plates, which serve as a relative weak point, and inherent characteristics of the osseous structures predispose the pediatric population to a unique pattern of injury. Interpreters of pediatric knee MRI must be cognizant of these differences as well as normal variations, such as the normal evolution of bone marrow signal with age and incidental yet inconsequential findings unique to this group, such as fibrous cortical defects.

MRI is widely used for evaluation of the knee as well as other joints and provides many advantages. These include lack of ionizing radiation; multiplanar imaging capabilities; excellent resolution; and superior evaluation of the soft tissues, bone marrow, cartilage, muscle, ligaments, and tendons. MRI protocols vary by institution; however, in general the knee should be imaged in three orthogonal planes (axial, sagittal, and coronal), and at least one sequence should be obtained with fat saturation and one without. Our standard protocol for knee trauma or pain includes a sagittal proton density sequence without fat saturation and sagittal, coronal, and axial proton density images with fat saturation. Images are obtained at a 3-mm slice thickness with a 1-mm interslice gap. A 3D sagittal water-selective excitation sequence or 3D spoiled gradient-recalled echo with fat saturation sequence provides excellent assessment of the articular and physeal cartilage. Although not a focus of this article, imaging protocols for suspected tumor or infection at the knee will differ and include T1-weighted imaging and gadolinium-enhanced T1-weighted imaging with fat saturation. The purpose of this review article is to highlight the key MRI features encountered in pediatric knee trauma.

Menisci

One of the most commonly reported internal derangements in a skeletally immature knee is a meniscal injury; however, the incidence of meniscal tears is significantly less than compared with the adult population [1]. Although meniscal injuries are commonly associated with ligamentous injuries, meniscal injuries are more frequently reported than anterior cruciate ligament (ACL) injuries in a pediatric population. The medial meniscus is more frequently injured than the lateral meniscus and the posterior horn more commonly than the anterior horn. A strong correlation exists between MR evaluation of meniscal tears and surgical findings, with sensitivity of 80–85% and specificity of 88–100% reported in one study [1].

Meniscal signal characteristics have been widely accepted for use in the adult population and can also be used in the pediatric population [2, 3]. Grade 1 refers to the uniformly low normal meniscal signal, grade 2 describes increased signal within the meniscus that does not extend to an articular surface, and grade 3 refers to abnormal signal extending to an articular surface indicative of a tear. In adults, grade 2 meniscal signal has been attributed to myxoid degeneration; however, in the pediatric population, grade 2 signal may relate to persistent vasculature [4].

There are multiple types of meniscal tears, including horizontal, vertical, bucket-handle, radial, peripheral, and displaced flap tears. A patient with a bucket-handle tear typically presents with locking and requires surgical attention. A bucket-handle tear is a longitudinally oriented tear of the meniscus with the torn fragment flipped centrally into the intercondylar notch; described imaging signs of bucket-handle tear include the double posterior cruciate ligament (PCL) sign and a displaced fragment of the meniscus in the coronal plane [5] (Fig. 1). The absent bowtie sign has been described by Helms et al. [6, 7]; this sign describes the absence of the normal configuration of the meniscus on the sagittal plane. Specifically, on sagittal imaging of the knee from peripheral to central, the body of the meniscus should be identified on at least two consecutive 4- to 5-mm-thick images and should have a bowtie configuration. However, this sign may not be as reliable in the pediatric population because the size of the meniscus will vary with age, and the bowtie sign is described in the adult meniscus, which is approximately 9–12 mm in width [6, 7].

A discoid meniscus is a common variant describing an abnormally enlarged meniscal body (Fig. 2). A spectrum of abnormality exists. This has been reported to occur in up to 10% of the pediatric population but in clinical practice is much less common [8, 9]. Discoid menisci are almost uniformly lateral. A two to one female to male predominance has been reported. The discoid meniscus has been associated with degeneration and tearing because of its abnormal shape and altered mechanics [10]. The discoid meniscus can be asymptomatic or symptomatic with pain and locking or "clunking." Children with lateral discoid meniscus may present with snapping knee syndrome in which the knee snaps with flexion and extension; however, this presentation is usually seen in the Wrisberg type of discoid meniscus, which is hypermobile because of lack of a posterior tibial attachment [11–13]. Children with discoid menisci most often present between 10 and 15 years of age when symptoms occur [8, 14]. Isolated tears of the lateral meniscus, particularly in younger children, should raise suspicion for an underlying discoid meniscus.

The criteria for diagnosis include visualization of the meniscal body on at least three or more 4- to 5-mm contiguous sagittal images, at least 2 mm or greater measurable height difference between the discoid and normal meniscus on the coronal plane, or greater than 12 mm in width [15].

A discoid meniscus has been associated with other anomalies, including a high fibular head, hypoplasia of the lateral tibial femoral condyle and tibial spine, and lateral joint space widening [15]. Meniscal cysts are also associated with discoid menisci; however, they are otherwise uncommonly seen in the pediatric population [2].

Cruciate Ligaments

ACL injuries are frequent in the adolescent population, more prevalent in girls and those of both sexes who are active in sports [16]. Reported contributing factors to female predominance include joint laxity, hormonal factors, limb alignment, configuration of the intercondylar notch, ligament size, and possibly earlier physeal fusion [17, 18]. The accuracy of MRI for detecting meniscal and ACL tears in adolescents is comparable with that of adults but is reportedly less accurate in patients before physeal closure [19].

Primary and secondary signs of ACL tears in children have been described and are similar to those seen in adults. Primary signs include fiber discontinuity, altered course, and abnormal signal of the ligament [20] (Fig. 3). Secondary signs include increased angle and abnormally vertical orientation of the PCL, anterior tibial displacement, uncovering of the posterior horn of the lateral meniscus, and kissing contusions of the lateral femoral condyle and medial tibial plateau [18, 20]. This pattern of bone marrow edema has been reported in skeletally immature patients even without an ACL tear, which may be secondary to increased laxity of the ACL in this population [21] in contrast with adult patients in whom ACL tears are consistently seen with this pattern of osseous contusion. Sensitivity of 95% and specificity of 88% in detecting ACL tears in children have been reported by Lee et al. [18] using both primary and secondary signs. Those authors found that primary findings were most reliable in diagnosing tears. In addition, this study discovered that meniscal tears were frequently associated with ACL injuries in children, more so than has previously reported in an adult population [18]. Fractures associated with ACL tears are avulsion of the lateral tibial rim at the insertion of the capsular ligament (Segond fracture), subchondral impaction fracture of the lateral femoral condyle, and avulsion of the tibial spine; however, these findings are not sensitive for diagnosis of ACL injuries [22].

Partial ACL tears are more common in the skeletally immature patient than the skeletally mature population [23]. This has been attributed to the relatively weaker bone at the ligament attachment site compared with the ligament itself. As the skeleton matures and growth plates fuse, the fused osseous structures are relatively stronger compared with the ligament, and therefore stresses on the knee result in a higher frequency of ligament tears compared with avulsions [23]. Differentiating partial from complete tears is critical because partial tears can be treated conservatively, whereas complete tears may need operative management. ACL reconstruction is a controversial topic because repair may lead to inadvertent injury to the femoral or tibial growth plates, resulting in premature physeal fusion and subsequent leg length discrepancies [24]. Physeal sparing procedures are typically performed in the younger population [24].

PCL injuries are uncommon in the pediatric population, but may occur with hyperextension injuries or with severe multiligamentous injury from knee dislocation. Hyperextension injuries of the knee may also result in avulsions of the posterior tibial plateau at the insertion site of the PCL without a tear of the PCL itself [25]. Similar to ACL tears, a PCL tear is diagnosed when there is disruption of fibers, increased signal intensity of the ligament, and redundancy of an avulsed ligament [26] (Fig. 4). Isolated PCL tears are rare and tears usually occur in the company of other ligamentous injuries [25]. Contusions of the anterior tibia and femur may be seen because of the hyperextension mechanism.

Collateral Ligaments

In the pediatric population, medial collateral ligament (MCL) and lateral collateral ligament (LCL) complex injuries are relatively uncommon compared with meniscal and ACL injuries. Similar to the adult population, collateral ligament injuries are seen in association with cruciate ligament and meniscal injuries [1, 3]. Injury to the MCL occurs secondary to valgus stress with the knee in a flexed position [27]. MCL and LCL injuries are classified as grades 1–3: grade 1 refers to microscopic injury; grade 2, to a partial tear; and grade 3, a complete tear [28]. On MRI, grade 1 is an intact ligament with variable amounts of surrounding edema, grade 2 is a ligament that is thickened or has abnormal signal with surrounding edema, and grade 3 is complete disruption of the fibers with surrounding edema (Fig. 5).

Bone and Cartilage

Before physeal fusion, the growth plates remain relatively weak and are a potential site of injury. Physeal injuries have been reported in up to 2.9% of pediatric knee MRI examinations [29]. Most physeal fractures are clinically suspected and radiographically evident; however, some physeal fractures can be subtle or radiographically occult, particularly those of the distal femur. MRI can be particularly helpful in these cases [29]. Evaluation of the physis should be part of the standard search pattern when interpreting knee MRI in the pediatric population. A Salter-Harris type II fracture is the most common type of physeal fracture and is also the most common fracture diagnosed on MRI [29]; linear abnormal signal intensity is identified in the metaphysis extending into the physis with associated widening of the growth plate (Fig. 6). Periosteal interruption or elevation can be seen with Salter-Harris II fractures, for which periosteal disruption is characteristically seen on the physeal fracture side of the growth plate as opposed to the metaphyseal side of the fracture [29]. Periosteal elevation may be seen on both sides. Uncommonly, avulsed periosteum may become entrapped within a physeal fracture [30].

Physeal widening because of stress injury has been reported in skeletally immature high-performance athletes [31]. These areas of physeal widening are thought to be secondary to repetitive stress and differ from Salter-Harris type I fractures, which result from acute injury [31]. With this type of chronic injury, a fracture line is not identified and the widening can be focal (Fig. 7).

Before physeal closure, avulsions of the tibial spine are not rare. In most cases, the ACL is intact but tibial spine avulsions may occur in association with ACL tears (Fig. 8). These patients can clinically present with an ACL-deficient knee, although the fibers remain intact [32]. The tibial spine is relatively weaker than the ACL in children and the configuration of the intercondylar notch has been implicated as a contributing factor to this injury, and those patients with a wider intercondylar notch may be predisposed to tibial avulsion fractures [33]. Tibial spine avulsion injuries may be radiographically subtle or occult and may be initially detected with MRI. Fortunately, because the ACL is usually intact, surgical repair of an avulsed tibial spine is usually simple and effective.

Chondral and osteochondral injuries were the most common lesions discovered in children undergoing MRI for evaluation of internal derangement of the knee in one study [34]. This study determined that chondral injuries were more frequently detected compared with meniscal and ACL injuries, and patterns varied depending on stage of physeal closure. Although the prevalence of chondral injuries did not change significantly with skeletal maturity, the pattern of chondral injury did. Before physeal closure, chondral injury of the femur was more commonly identified compared with patellar chondral injury after growth plate fusion. Subchondral bone marrow edema was a common associated finding [34]. Chondral injuries are considered significant because they may predispose to premature osteoarthritis and, if producing a loose fragment within the joint, may cause locking and pain [34]. Fat-suppressed spoiled gradient-echo MR sequences and sagittal water-selective excitation sequences are useful to assess cartilage.

Osteochondritis dissecans (OCD) is an acquired condition in which an osteochondral fragment partially or completely dislodges from the articular surface. Although this condition is likely posttraumatic in cause, other theories include repetitive mechanical stress, congenital factors, avascular necrosis, and even fat emboli [35]. The medial femoral condyle is the most affected (85% of cases); however, the inferocentral lateral femoral condyle, anterior lateral femoral condyle, femoral sulcus, and the patella can also be affected [36] (Fig. 9).

OCD may be diagnosed with radiography and seen as a focal lucency involving subchondral bone, often containing a central osseous fragment and variable degrees of surrounding sclerosis [37]. However, MRI is useful in assessing stability of the lesion, which has surgical implications because loose or displaced fragments require surgical management. Mesgarzadeh et al. [38] reported that MRI was 92% sensitive and 90% specific for separating stable from loose lesions. MR signs of instability have been described. These signs are presence of a high-signal-intensity line along the fragment interface, disruption of the subchondral bone plate, and a 5-mm or larger fluid-filled cyst adjacent to the lesion [39]. Those with displaced fragments had the osseous defects filled with joint fluid [39]. Findings associated with good clinical outcome include stability of the lesion, small size of the OCD, and open growth plates [37]. Articular defect or cartilage fracture was associated with a poor outcome [37]. MRI criteria may have less specificity for instability in skeletally immature patients [40].

OCD must be differentiated from normal variants of ossification, most commonly seen along the posterior aspect of the lateral femoral condyle. Ossification defects in these areas with intact overlying cartilage and lack of bone marrow edema are features supportive of developmental variants [41] (Fig. 9).

Patella and Patellar Tendon

Traumatic patellar dislocation is a common acute knee injury in children, but it is often transient and occult and not suspected at the time of initial clinical or radiographic evaluation [42]. Typically, there is a complete, usually lateral, displacement of the patella out of the femoral groove and relocation, which is often spontaneous and not recognized. Indirect signs include hemarthrosis, contusion or osteochondral injury of the medial patellar facet and lateral femoral condyle, and injury to the medial patellar retinaculum [42] (Fig. 10). Predisposing factors include genu valgum, ligamentous laxity, shallow femoral trochlea, and abnormal morphology of the patellar facets.

Acute avulsion of the cartilage of the inferior patellar pole with an underlying bone fragment is termed “patellar sleeve fracture” and occurs most commonly in the 8- to 12-year-old population. Although radiographic and MR findings are similar and include joint effusion, avulsed osseous fragment, and patella alta, MRI can identify the true extent of injury, including the presence of a nondisplaced osteochondral fracture, the extent of soft-tissue injury, and the need for operative management [43, 44] (Fig. 11). Chronic avulsion injury of the inferior patellar pole is termed “Sinding-Larsen-Johansson syndrome.” MRI is also useful to determine the extent of findings, including fragmentation of the inferior patellar pole, infiltration of Hoffa fat-pad, and thickening of the proximal patellar tendon [45] (Fig. 11). Calcification or ossification of the tendon can also be identified.

Chronic avulsion or overuse injuries can also involve the tibial tubercle, termed "Osgood-Schlatter disease." The tibial tubercle is an anterior extension of the tibial physis and is prone to injury because of its unique composition, which varies from other physes [43]. As the tibial tubercle matures, its susceptibility to injury from stresses incurred by the patellar tendon increases. Repetitive stress on the tibial tubercle by the patellar tendon causes inflammation at the patellar tendon insertion site, reactive bone formation, bone marrow edema, proximal patellar tendon thickening, and soft-tissue swelling (Fig. 12). Although Osgood-Schlatter disease is a clinical diagnosis, MRI is useful in characterizing these changes, especially in the early stage of disease when only bone marrow edema may be present adjacent to the tibial tuberosity [46]. Osgood-Schlatter disease may predispose to avulsion fractures of the tibial tubercle, which also may be seen as an acute injury, most commonly in teenage boys involved in jumping sports [43]. When osseous irregularity is seen at this site in the absence of other findings and symptoms, irregularity of the ossification center must be considered as a normal variant.

Patellar variants are also encountered with imaging. Bipartite patella is a failure of fusion of a secondary ossification center of the patella, usually at the superolateral aspect of the patella [45]. This normal variant is usually asymptomatic; however, acute or chronic stress injuries may disrupt the synchondrosis between the accessory ossification center and patella, causing symptoms [47].

Incidental Findings and Normal Variations

Neoplasms and tumorlike conditions may present with pain, pathologic fracture, or be incidentally discovered during evaluation of the pediatric knee. Lesions include chondroblastomas, giant cell tumors, osteochondromas, osteoid osteomas, fibrous cortical defects or nonossifying fibromas, and cortical desmoids [48].

Fibrous cortical defects and nonossifying fibromas are well-defined cortically based lobulated lesions with sclerotic margins on radiography. Unless a pathologic or stress fracture is present, there will be no associated pain, edema, or periostitis. By definition, a lesion under 2 cm in size is a fibrous cortical defect and a lesion 2 cm or greater is a nonossifying fibroma (Fig. 13). The lesions are histologically identical. MRI and radiographic appearances are variable and relate to the stage of evolution. The lesions show T2 hyperintensity early during development; however, as they involute, the T2 signal decreases or becomes undetectable [48] (Fig. 13). Involuting lesions are low signal on all sequences because of sclerosis. Lesions are well defined, lobular or unilocular, and cortically based. Edema is not identified with uncomplicated lesions, but edema may occasionally be seen with an associated stress fracture.

Avulsive cortical irregularities and so called cortical desmoids are commonly seen at the posteromedial distal femoral diaphysis (Fig. 13). These are thought to be secondary to chronic traction at the femoral insertion site of the medial head of the gastrocnemius or adductor magnus aponeurosis [49]. Cortical desmoids are focal well-defined scalloped lesions along the cortical surface that are typically T1 hypointense and T2 hyperintense, with marginal sclerosis. A cortical desmoid disrupts the cortex from the outer surface and does not change in position over time [49]. In contrast, a fibrous cortical defect typically erodes the cortex from within the bone and tends to migrate proximally over time. Histologically, cortical desmoids and fibrous cortical defects are similar if not identical.

The normal evolution of bone marrow must also be considered when interpreting any MRI. The signal of bone marrow reflects the relative amounts of yellow and red marrow and their relative composition of fat, water, and protein [50]. Starting at birth, a normal pattern of conversion from red to yellow marrow takes place, which begins peripherally and progresses centrally; understanding this normal evolution is essential if marrow pathology is to be detected. Residual hematopoietic marrow in the distal femoral metaphysis may appear inhomogeneous.

Conclusion

The injury patterns in the pediatric knee both overlap and differ from the adult. Differences between the adult and pediatric populations include an open physis, which serves as a relative point of weakness before physeal fusion; changing mechanics; and differences in ligamentous support. When differences in pathology, disease prevalence, and mechanism of injury are acknowledged, a more accurate interpretation of the MRI findings can be rendered in the pediatric population. In addition, awareness and understanding of normal variants and normal evolution of bone marrow signal may aid in the interpretation of MRI and help avoid unnecessary further workup or intervention.

References

1. Zobel MS, Borrello JA, Siegel MJ, Stewart NR. Pediatric knee MR imaging: pattern of injuries in the immature skeleton. *Radiology* 1994; 190:397–401
2. King SJ. Magnetic resonance imaging of knee injuries in children. *Eur Radiol* 1997; 7:1245–1251
3. King SJ, Carty HM, Brady O. Magnetic resonance imaging of knee injuries in children. *Pediatr Radiol* 1996; 26:287–290
4. Crues JV 3rd, Mink J, Levy TL, Stoller DW. Meniscal tears of the knee: accuracy of MR imaging. *Radiology* 1987; 164:445–448
5. Stabler A, Glaser C, Reiser M. Musculoskeletal MR: knee. *Eur Radiol* 2000; 10:230–241
6. Helms CA. The meniscus: recent advances in MR imaging of the knee. *AJR* 2002; 179:1115–1122
7. Helms CA, Laorr A, Cannon WD Jr. The absent bow tie sign in bucket-handle tears of the menisci in the knee. *AJR* 1998; 170:57–61
8. Stark JE, Siegel MJ, Weinberger E, Shaw DW. Discoid menisci in children: MR features. *J Comput Assist Tomogr* 1995; 19:608–611
9. Ryu KN, Kim IS, Kim EJ, et al. MR imaging of tears of discoid lateral menisci. *AJR* 1998; 171:963–967
10. Woods GW, Whelan JM. Discoid meniscus. *Clin Sports Med* 1990; 9:695–706
11. Rubin DA. MR imaging of the knee menisci. *Radiol Clin North Am* 1997; 35:21–44
12. Kelly BT, Green DW. Discoid lateral meniscus in children. *Curr Opin Pediatr* 2002; 14:54–61
13. Singh K, Helms CA, Jacobs MT, Higgins L. MRI appearance of Wrisberg variant of discoid lateral meniscus. *AJR* 2006; 187:384–387
14. Davidson D, Letts M, Glasgow R. Discoid meniscus in children: treatment and outcome. *Can J Surg* 2003; 46:350–358
15. Silverman JM, Mink JH, Deutsch AL. Discoid menisci of the knee: MR imaging appearance. *Radiology* 1989; 173:351–354
16. Micheli LJ. Pediatric and adolescent sports injuries: recent trends. *Exerc Sport Sci Rev* 1986; 14:359–374
17. Huston LJ, Greenfield ML, Wojtys EM. Anterior cruciate ligament injuries in the female athlete: potential risk factors. *Clin Orthop Relat Res* 2000; 372:50–63
18. Lee K, Siegel MJ, Lau DM, Hildebolt CF, Matava MJ. Anterior cruciate ligament tears: MR imaging based diagnosis in a pediatric population. *Radiology* 1999; 213:697–704
19. McDermott MJ, Bathgate B, Gillingham B, Hennrikus W. Correlation of MRI and arthroscopic diagnosis of knee pathology in children and adolescents. *J Pediatr Orthop* 1998; 18:675–678
20. Brandser EA, Riley MA, Berbaum KS, El-Khoury GY, Bennett DL. MR imaging of anterior cruciate ligament injury: independent value of primary and

secondary signs. *AJR* 1996; 167:121–126

21. Snearly WN, Kaplan PA, Dussault RG. Lateral compartment bone contusions in adolescents with intact anterior cruciate ligaments. *Radiology* 1996; 198:205–208
22. Matherne TH, Monu JU, Schruff L, Neitzschman HR. Avulsions around the knee portend instability. *Emerg Radiol* 2005; 11:213–218
23. Prince JS, Laor T, Bean JA. MRI of anterior cruciate ligament injuries and associated findings in the pediatric knee: changes with skeletal maturation. *AJR* 2005; 185:756–762
24. Shea KG, Apel PJ, Pefeiffer RP. Anterior cruciate ligament injury in paediatric and adolescent patients. *Sports Med* 2003; 33:455–471
25. Sonin AH, Fitzgerald SW, Hoff FL, Friedman H, Bresler ME. MR imaging of the posterior cruciate ligament: normal, abnormal and associated injury patterns. *RadioGraphics* 1995; 15:551–556
26. Grover JS, Bassett LW, Gross ML, Seeger LL, Finerman GA. Posterior cruciate ligament: MR imaging. *Radiology* 1990; 174:527–530
27. Scweitzer ME, Tran D, Deely DM, Hume EL. Medial collateral ligament injuries: evaluation of multiple signs, prevalence and location of associated bone bruises, and assessment with MR imaging. *Radiology* 1995; 194:825–829
28. Cham KM, Hsu CYC. Cartilage and ligament injuries in sports. In: Renstrum PA, ed. *Clinical practice of sports injury prevention and care*. London, UK: Oxford University Press, 1993:54–70
29. Close BJ, Strouse PJ. MR of physeal fractures of the adolescent knee. *Pediatr Radiol* 2000; 30:756–762
30. Whan A, Breidahl W. Janes G. MRI of trapped periosteum in a proximal tibial physeal injury of a pediatric patient. *AJR* 2003; 181:1397–1399
31. Laor T, Wall EJ, Vu LP. Physeal widening in the knee due to stress injury in child athletes. *AJR* 2006; 186:1260–1264
32. Delzell PB, Schils JP, Recht MP. Subtle fractures about the knee: innocuous-appearing yet indicative of significant internal derangement. *AJR* 1996; 167:699–703
33. Kocher MS, Mandiga R. Klingele, Bley L, Micheli LJ. Anterior cruciate ligament injury versus tibial spine fracture in the skeletally immature knee: a comparison of skeletal maturation and notch width index. *J Pediatr Orthop* 2004; 24:185–188
34. Oeppen RS, Connolly SU, Bencardino JT, Jaramillo D. Acute injury of the articular cartilage and subchondral bone: a common but unrecognized lesion in the immature knee. *AJR* 2004; 182:111–117
35. Mitsuoka T, Shino K, Hamada M, Horibe S. Osteochondritis dissecans of the lateral femoral condyle of the knee joint. *Arthroscopy* 1999; 15:20–26
36. Boutin RD, Januario JA, Newburg AH, Gundry CR, Newman JS. MR imaging features of osteochondritis dissecans of the femoral sulcus. *AJR* 2003; 180:641–645
37. De Smet AA, Hai OA, Graf BK. Untreated osteochondritis dissecans of the femoral condyles: prediction of patient outcome using radiographic and MR findings. *Skeletal Radiol* 1997; 26:463–467
38. Mesgarzadeh M, Sapega A, Bonakdarpour A, et al. Osteochondritis dissecans: analysis of mechanical stability with radiography, scintigraphy and MR imaging. *Radiology* 1987; 165:775–780
39. De Smet AA, Fisher DA, Graf BK, Lange RH. Osteochondritis dissecans of the knee: value of MR imaging in determining lesion stability and the presence of articular cartilage defects. *AJR* 1990; 155:549–553
40. Kijowski R, Blankenbaker DG, Shinki K, Fine JP, Graf BK, De Smet AA. Juvenile versus adult osteochondritis dissecans of the knee: appropriate MR imaging criteria for instability. *Radiology* 2008; 248:571–578
41. Gebarski K, Hernandez R. Stage-1 osteochondritis dissecans versus normal variants of ossification in children. *Pediatr Radiol* 2005; 35:880–886
42. Zaidi A, Babyn P, Astori I, White L, Doria A, Cole W. MRI of traumatic patellar dislocation in children. *Pediatr Radiol* 2006; 36:1163–1170
43. Dupuis CS, Westra SJ, Makris J, Wallace EC. Injuries and conditions of the extensor mechanism of the pediatric knee. *RadioGraphics* 2009; 29:877–886
44. Bates DG, Hresko MT, Jaramillo D. Patellar sleeve fracture: demonstration with MR imaging. *Radiology* 1994; 193:825–827
45. Dwek JR, Chung CB. The patellar extensor apparatus of the knee. *Pediatr Radiol* 2008; 38:925–935
46. Hirano A, Fukubayashi T, Ishii T, Ochiai N. Magnetic resonance imaging of Osgood-Schlatter disease: the course of the disease. *Skeletal Radiol* 2002; 31:334–342
47. Kavanagh EC, Zoga A, Omar I, Ford S, Schweitzer M, Eustace S. MRI findings in bipartite patella. *Skeletal Radiol* 2007; 36:209–214
48. Stacy GS, Heck RK, Peabody TD, Dixon LB. Neoplastic and tumorlike lesions detected on MR imaging of the knee in patients with suspected internal derangement. Part I. Intraosseous entities. *AJR* 2002; 178:589–594
49. Tyler P, Datir A, Saifuddin A. Magnetic resonance imaging of anatomical variations in the knee. Part 2. Miscellaneous. *Skeletal Radiol* 2010; 39:1175–1186
50. Siegel MJ. MR imaging of paediatric haematologic bone marrow disease. *J Hong Kong Coll Radiol* 2000; 3:38–50

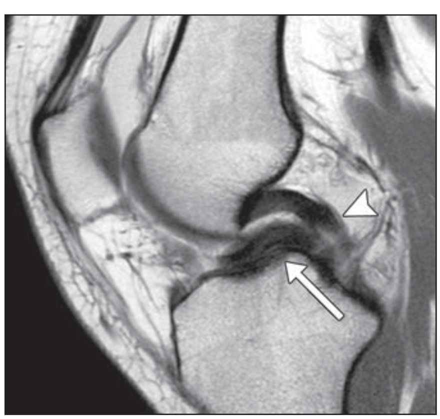

Fig. 1—17-year-old soccer player who twisted his knee. Sagittal proton density–weighted image through knee at level of posterior cruciate ligament (PCL) shows abnormal tissue (*arrow*) just deep in relation to normal PCL (*arrowhead*). This is example of double PCL sign and signifies bucket-handle tear of medial meniscus with flipped fragment.

Fig. 2—8-year-old boy with knee pain and no history of trauma. Coronal proton density–weighted image through knee shows discoid lateral meniscus with abnormal intrameniscal signal, compatible with degeneration (*arrow*).

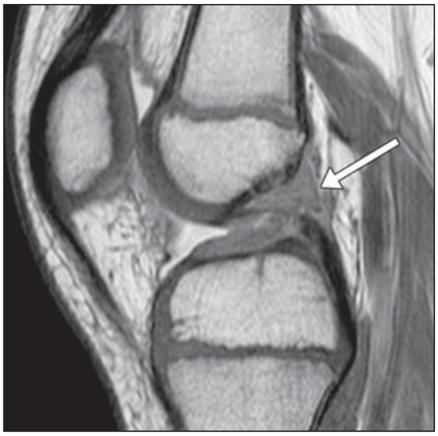

Fig. 3—9-year-old boy who injured his knee while playing football. Sagittal proton density–weighted image through knee shows fiber disruption and abnormal signal of anterior cruciate ligament, compatible with complete tear (*arrow*).

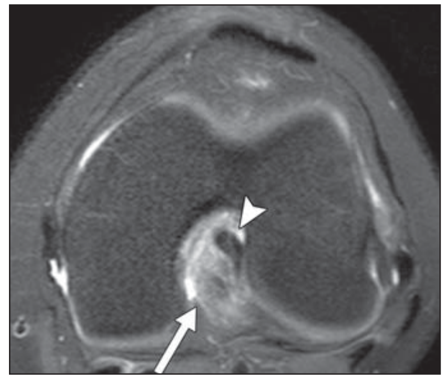

Fig. 4—14-year-old girl who injured her knee while jumping on trampoline. Axial proton density–weighted image with fat saturation through knee shows amorphous appearance and edema of posterior cruciate ligament, compatible with tear (*arrow*). Notice normal configuration and signal of anterior cruciate ligament located anteriorly (*arrowhead*).

A B C

Fig. 5—Collateral ligament injuries.
A, 13-year-old boy who was injured playing football. Coronal proton density–weighted image through knee shows abnormal fluid adjacent to intact medial collateral ligament (MCL), compatible with grade 1 injury (*arrow*).
B, 13-year-old boy who was struck by car. Coronal proton density–weighted image through knee shows disruption of lateral collateral ligament complex (*arrow*), with extensive surrounding edema. Findings are compatible with grade 3 injury.
C, 17-year-old football player who sustained direct trauma to lateral aspect of his knee. Coronal proton density–weighted image through knee shows complete tear of MCL, with wavy appearance of ligament distally and surrounding fluid (*arrow*). Associated anterior cruciate ligament tear was identified (*arrowhead*). This patient also had bone marrow edema of lateral femoral condyle.

Fig. 6—17-year-old soccer player who was kicked during practice. Coronal proton density–weighted image through knee with fat saturation shows linear signal intensity extending from distal femoral metadiaphysis through medial physis, compatible with Salter-Harris type II fracture (*arrow*). Note adjacent bone marrow edema and disruption of periosteum (*arrowhead*). Joint effusion is also seen.

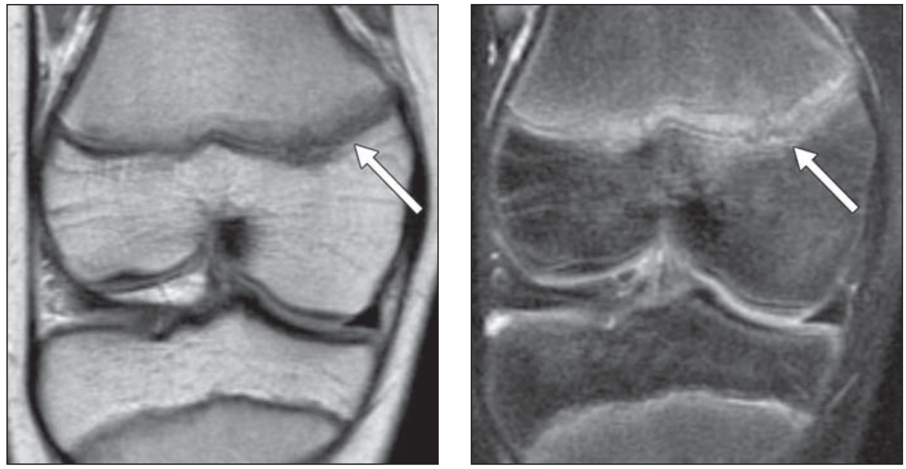

A B

Fig. 7—12-year-old soccer player with knee pain.
A, Coronal proton density–weighted image through knee shows widening and indistinct appearance of medial distal femoral physis, compatible with stress injury of growth plate (*arrow*).
B, Coronal proton density–weighted image with fat saturation through knee shows similar findings, with mild edema along margins of physis (*arrow*).

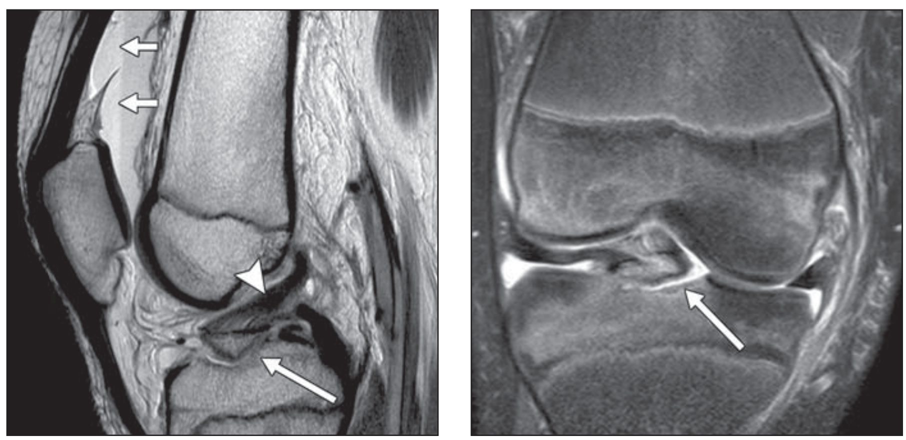

A B

Fig. 8—13-year-old boy who felt his knee "give out" while being tackled by another player during football practice.
A, Sagittal proton density–weighted image through knee at level of anterior cruciate ligament (ACL) shows avulsion fracture of tibial spine with bone marrow edema (*long arrow*). The ACL (*arrowhead*) is intact, as it often is with this fracture. Fluid–fluid level of hemarthrosis is also noted (*short arrows*).
B, Coronal proton density–weighted image with fat saturation through knee shows bone marrow edema of avulsed tibial spine (*arrow*).

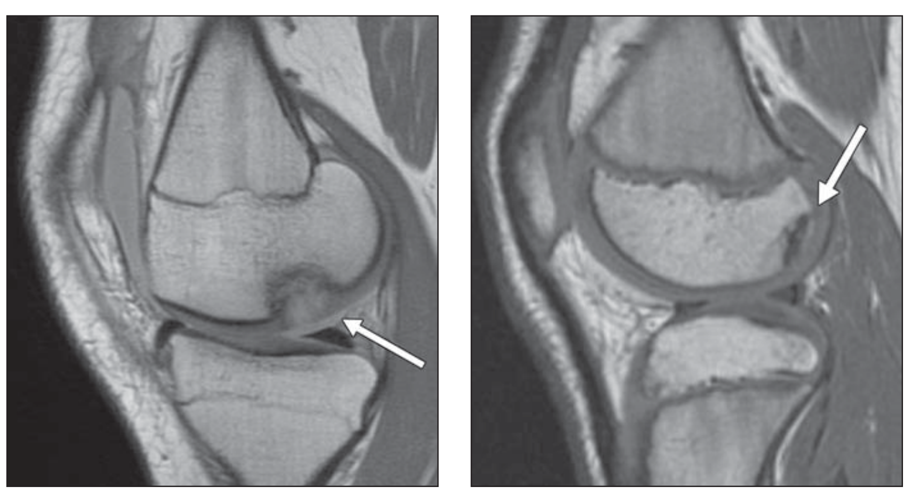

A B

Fig. 9—Osteochondritis dissecans (OCD) and normal variant mimicking OCD.
A, Sagittal proton density–weighted image of knee of 15-year-old girl shows abnormal subchondral marrow signal involving weightbearing aspect of medial femoral condyle with overlying cartilage irregularity, compatible with OCD (*arrow*). Joint effusion is also present.
B, Contrast-enhanced sagittal proton density–weighted image through knee of 9-year-old boy shows hypointense signal alterations within posterior aspect of medial femoral condyle with normal appearing overlying cartilage (*arrow*). This is example of normal developmental variant.

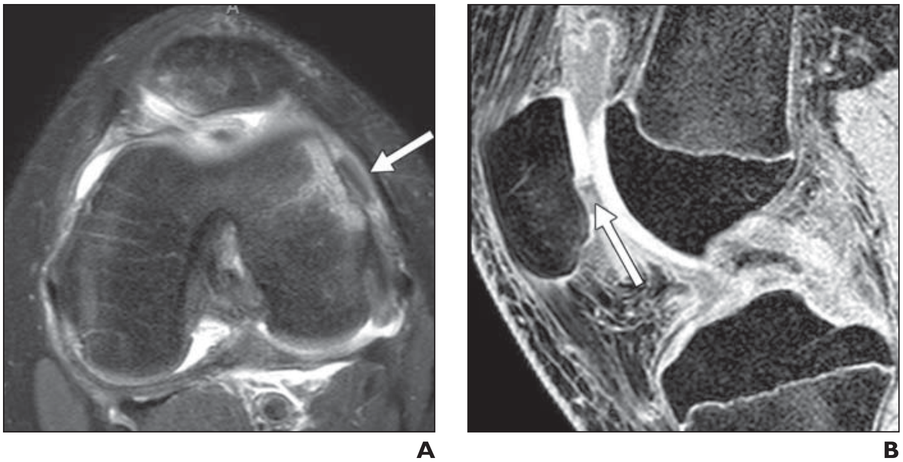

Fig. 10—14-year-old football player tackled during practice who presented with anterior knee pain.
A, Axial proton density–weighted image with fat saturation through level of patella shows contusions of lateral femoral condyle and medial patellar facet, edema and injury to medial patellar retinaculum, and osteochondral fragment (*arrow*) within lateral joint recess, compatible with transient patellar dislocation.
B, Sagittal water-selective excitation sequence through knee shows osteochondral defect (donor site) from inferior patella (*arrow*).

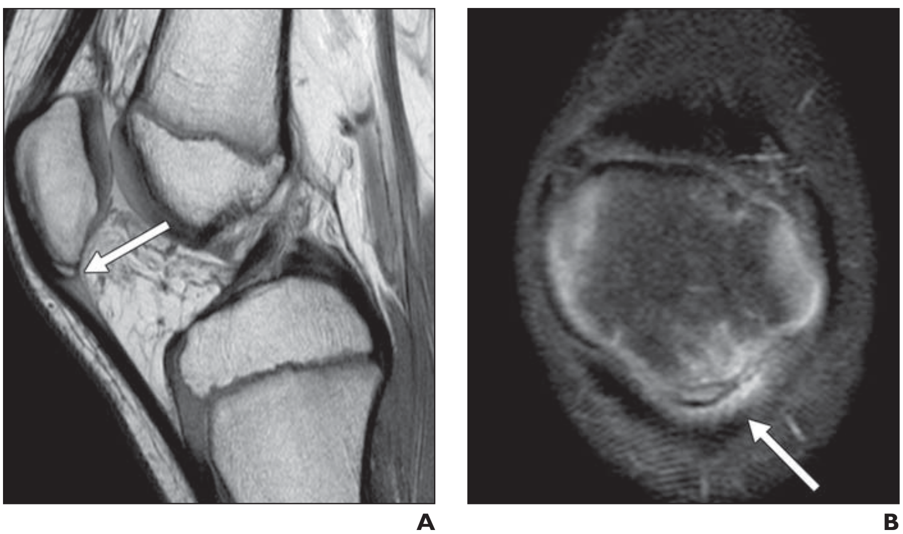

Fig. 11—Inferior patellar pole.
A, Sagittal proton density–weighted image through knee of 12-year-old basketball player shows fracture of inferior patellar pole, compatible with patellar sleeve injury (*arrow*).
B, Coronal proton density–weighted image with fat saturation through knee of another 12-year-old basketball player shows fragmentation of inferior patellar pole (*arrow*) with associated bone marrow edema and mild thickening of proximal patellar tendon. Findings are compatible with Sinding-Larsen-Johansson syndrome and traction apophysitis at level of proximal patellar tendon.

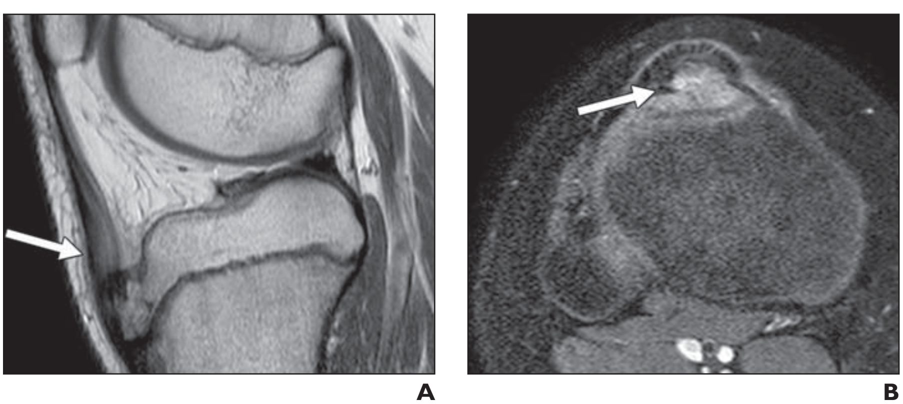

Fig. 12—11-year-old boy with knee pain.
A, Sagittal proton density–weighted image through knee shows fragmentation of tibial tubercle, with overlying soft-tissue swelling and thickening and abnormally increased signal of distal patellar tendon (*arrow*).
B, Axial proton density–weighted image with fat saturation through level of distal patellar tendon shows thickening and abnormally increased signal (*arrow*). Findings are compatible with Osgood-Schlatter disease.

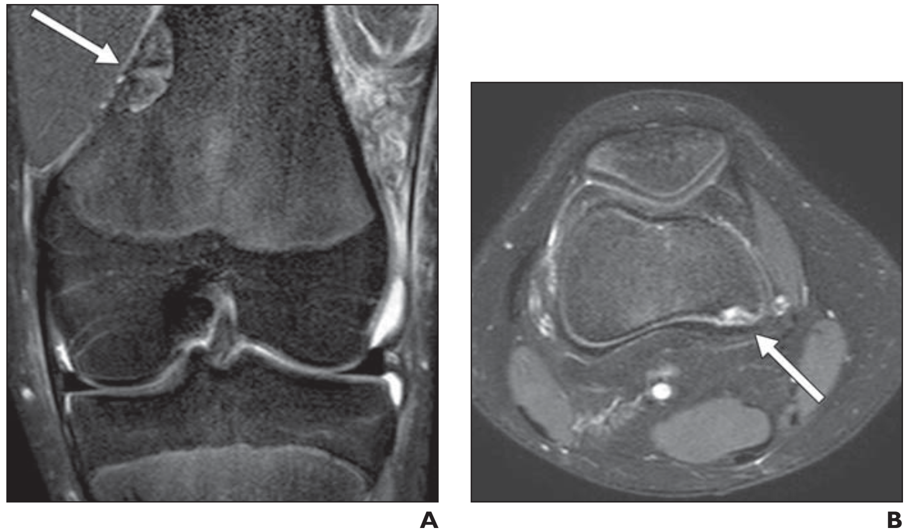

Fig. 13—Fibrous cortical defect and cortical desmoid.
A, Coronal proton density–weighted image with fat saturation in 15-year-old boy shows cortically based lobulated heterogeneously hyperintense lesion along distal femoral metadiaphysis measuring less than 2 cm, compatible with fibrous cortical defect (*arrow*).
B, Axial proton density–weighted image with fat saturation of 13-year-old girl shows cortically based lobulated hyperintense lesion involving posteromedial distal femoral metadiaphysis near adductor magnus aponeurosis, compatible with cortical desmoid (*arrow*).

FOR YOUR INFORMATION

This article is available for CME credit. See www.arrs.org for more information.